

Computational Modeling of Vesicle Release in the Retina

Benjamin Leung

August, 3, 2009

Abstract

This report examines an existing model of neurotransmitter release in photoreceptors and bipolar cells, and implements them into a MATLAB program using a system of Linear ODEs. In addition, the model was expanded to include a new calcium dependency present in the final vesicle fusing stage. This calcium dependency also had a number of potential models, and each were programmed in and compared qualitatively to each other and data from laboratory. Finally, the models were implemented into a graphical user interface for ease-of-use.

1 Introduction

Photoreceptors and bipolar cells in the retina are unique due to their graded response to stimulus, rather than the usual integrate and fire mechanism. This form of release is needed because those cells are constantly releasing neurotransmitter even when receiving no outside stimulus. A specialized structure, a ribbon synapse, is needed to maintain this steady exocytosis by queuing up vesicles filled with neurotransmitter and fusing them with the membrane. In this report, a computational tool for analyzing this vesicle release is developed for future use by biologists.

2 Methods

A four pool model was previously theorized to accurately represent this graded release of neurotransmitter through the ribbon synapse [1], as shown in figure 1. Figure 2 shows a more graphical version of this setup. The depot pool consists of the vesicles scattered throughout the cell. The reserve pool is made of vesicles in the vicinity of the ribbon synapse. The remaining two pools contain the vesicles attached to the ribbon synapse; those that are nearest the membrane create the ultrafast pool.

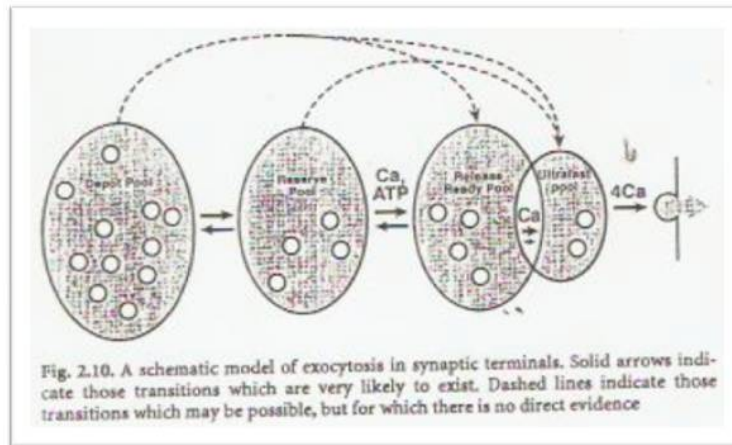


Figure 1. The four-pool model from [1].

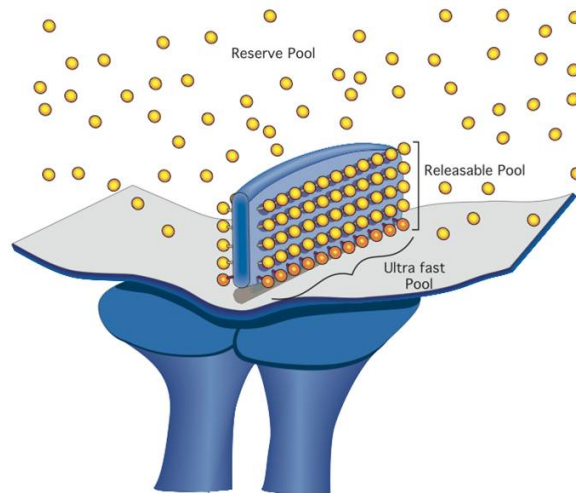


Figure 2. A graphical representation of the ribbon synapse.

However, the final fuse step requires a unique calcium dependency that the previous four pool model does not have [2][3], and thus the final step was initially implemented in a number of different fusion models. The models programmed in MATLAB were the five-site allosteric, the four-site conventional, the three-site conventional, and the two-site conventional. Two of the models are shown below.

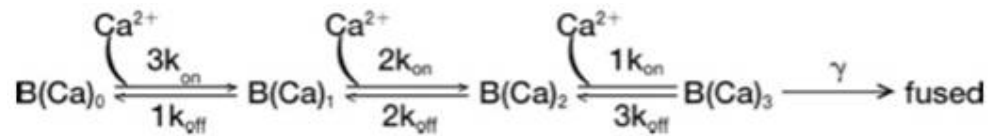


Figure 3. Three-site conventional fusion model [2].

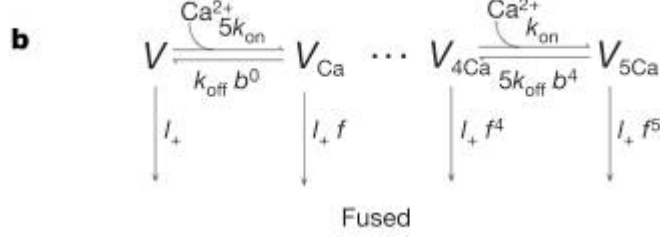


Figure 4. Five-site allosteric fusion model [3].

Each model can be represented by a system of linear ODEs:

Five site allosteric:

$$\begin{aligned} \frac{dbca0}{dt} &= -5(kon)(Ca)bca0 + (koff)bca1 - i(bca0) \\ \frac{dbca1}{dt} &= 5(kon)(Ca)bca0 + 2(koff)(b)bca2 - 4(kon)(Ca)bca1 - if(bca1) - \\ &(koff)bca1 \\ \frac{dbca2}{dt} &= 4(kon)(Ca)bca1 - 2(koff)(b)bca2 - 3(kon)(Ca)bca2 + 3(koff)(b^2)bca3 - \\ &i(f^2)bca2 \\ \frac{dbca3}{dt} &= 3(kon)(Ca)bca2 - 3(koff)(b^2)bca3 - 2(kon)(Ca)bca3 + 4(koff)(b^3)bca4 - \\ &i(f^3)bca3 \\ \frac{dbca4}{dt} &= 2(kon)(Ca)bca3 - d(koff)(b^3)bca4 + 5(koff)(b^4)bca5 - (kon)(Ca)bca4 - \\ &i(f^4)bca4 \\ \frac{dbca5}{dt} &= (kon)(Ca)bca4 - 5(koff)(b^4)bca5 - i(f^5)bca5 \\ \frac{dfused}{dt} &= i(bca0) + if(bca1) + i(f^2)bca2 + i(f^3)bca3 + i(f^4)bca4 + i(f^5)bca5 \end{aligned}$$

Four site conventional:

$$\begin{aligned} \frac{dbca0}{dt} &= (koff)bca1 - 4(kon)(Ca)bca0 \\ \frac{dbca1}{dt} &= 4(kon)(Ca)bca0 - (koff)bca1 - 3(kon)(Ca)bca1 + 2(koff)bca2 \\ \frac{dbca2}{dt} &= 3(kon)(Ca)bca1 - 2(koff)bca2 - 2(kon)(Ca)bca2 + 3(koff)bca3 \\ \frac{dbca3}{dt} &= 2(kon)(Ca)bca2 - 3(koff)bca3 - (kon)(Ca)bca3 + 4(koff)bca4 \\ \frac{dbca4}{dt} &= (kon)(Ca)bca3 - 4(koff)bca4 - \gamma bca4 \\ \frac{dfuse}{dt} &= \gamma bca4 \end{aligned}$$

Three site conventional:

$$\begin{aligned} \frac{dbca0}{dt} &= -3(kon)(Ca)bca0 + (koff)bca1 \\ \frac{dbca1}{dt} &= 3(kon)(Ca)bca0 - (koff)bca2 - 2(kon)(Ca)bca1 + 2(koff)bca2 \\ \frac{dbca2}{dt} &= 2(kon)(Ca)bca1 - 2(koff)bca2 - (kon)(Ca)bca2 + 3(koff)bca3 \\ \frac{dbca3}{dt} &= (kon)(Ca)bca2 - 3(koff)bca3 - \gamma bca4 \\ \frac{dfuse}{dt} &= \gamma bca4 \end{aligned}$$

Two site conventional

$$\begin{aligned} \frac{dbca0}{dt} &= -2(kon)(Ca)bca0 + (koff)bca1 \\ \frac{dbca1}{dt} &= 2(kon)(Ca)bca0 - (koff)bca1 - (kon)(Ca)bca1 + 2(koff)bca2 \\ \frac{dbca2}{dt} &= (kon)(Ca)bca1 - 2(koff)bca2 - \gamma bca2 \\ \frac{dfuse}{dt} &= \gamma bca2 \end{aligned}$$

Bca0, bca1, etc. denote the initial vesicle pool sizes.

kon is a rate constant for vesicles to move to faster pools.

koff is a rate constant for vesicles to move to slower pools.

Ca is the concentration of intraterminal calcium.

gamma is the vesicle fuse rate in the conventional models.

i is the instantaneous rate of fusion, representing the constant exocytosis of vesicles.

f is a multiplier constant to i, representing the greater rate of fusion from faster pools.

b is a multiplier constant that generally is between 0 and 1, and represents the increased difficulty in moving to slower pools.

In addition, the five-site allosteric model was combined with the original four pool model from the Heidelberger paper, yielding the following set of differential equations:

$$\begin{aligned}
\frac{dv_1}{dt} &= (k_{12r})v_2 - (k_{12})v_1 - (k_{14})v_1 - (k_{13})v_1 + (k_{51})v_5 \\
\frac{dv_2}{dt} &= (k_{12})v_1 - (k_{12r})v_2 + (k_{23r})v_3 - (k_{23})v_2 - (k_{24})v_3 \\
\frac{dv_3}{dt} &= (k_{23})v_2 - (k_{23r})v_3 - (k_{34})v_3 + (k_{34r})bca_0 + (k_{13})v_1 - (k_{35})v_3 \\
\frac{dbca_0}{dt} &= -5(kon)(Ca)bca_0 + (koff)bca_1 - i(bca_0) + (k_{34})v_3 + (k_{14})v_1 + \\
&(k_{24})v_2 - (k_{34r})bca_0 \\
\frac{dbca_1}{dt} &= 5(kon)(Ca)bca_0 + 2(koff)(b)bca_2 - 4(kon)(Ca)bca_1 - if(bca_1) - \\
&(koff)bca_1 \\
\frac{dbca_2}{dt} &= 4(kon)(Ca)bca_1 - 2(koff)(b)bca_2 - 3(kon)(Ca)bca_2 + 3(koff)(b^2)bca_3 - \\
&i(f^2)bca_2 \\
\frac{dbca_3}{dt} &= 3(kon)(Ca)bca_2 - 3(koff)(b^2)bca_3 - 2(kon)(Ca)bca_3 + 4(koff)(b^3)bca_4 - \\
&i(f^3)bca_3 \\
\frac{dbca_4}{dt} &= 2(kon)(Ca)bca_3 - d(koff)(b^3)bca_4 + 5(koff)(b^4)bca_5 - (kon)(Ca)bca_4 - \\
&i(f^4)bca_4 \\
\frac{dbca_5}{dt} &= (kon)(Ca)bca_4 - 5(koff)(b^4)bca_5 - i(f^5)bca_5 \\
\frac{dfused}{dt} &= i(bca_0) + if(bca_1) + i(f^2)bca_2 + i(f^3)bca_3 + i(f^4)bca_4 + i(f^5)bca_5 - \\
&(k_{51})fused + (k_{35})v_3
\end{aligned}$$

3 Results

The previous were implemented into a graphical user interface. Figure 5 shows the GUI for just the final fuse step, while figure 6 shows the GUI for the four pool combined with the five site allosteric.



Figure 5. The fuse step GUI.

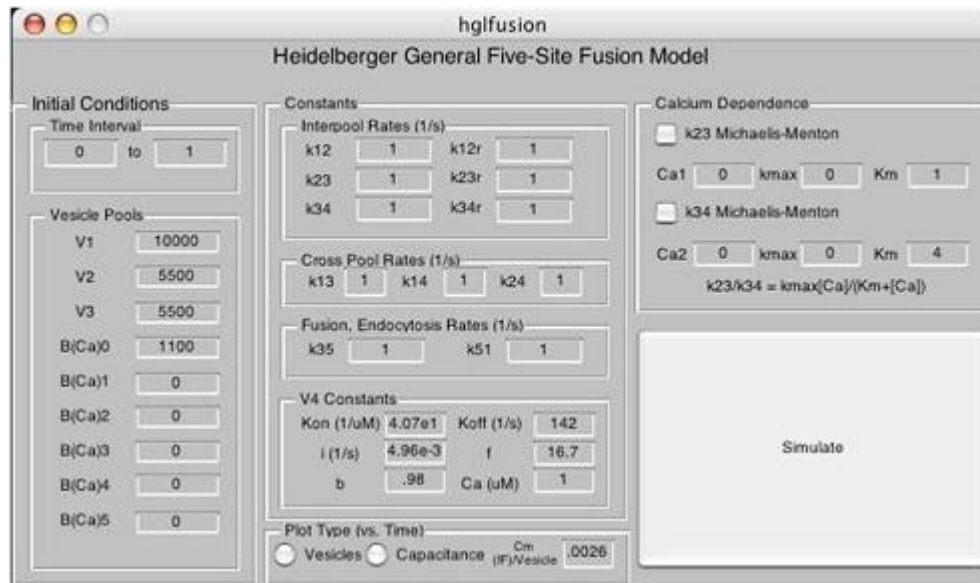


Figure 6. The combined model GUI.

Initial pool sizes were taken from accepted data for the goldfish bipolar cell. Rate constants were taken from lab data for the salamander rod photoreceptor, as the lab had no established values yet. But as long as the parameters used were consistent, it should not matter. Below are the resulting graphs from each of the different fusion models:

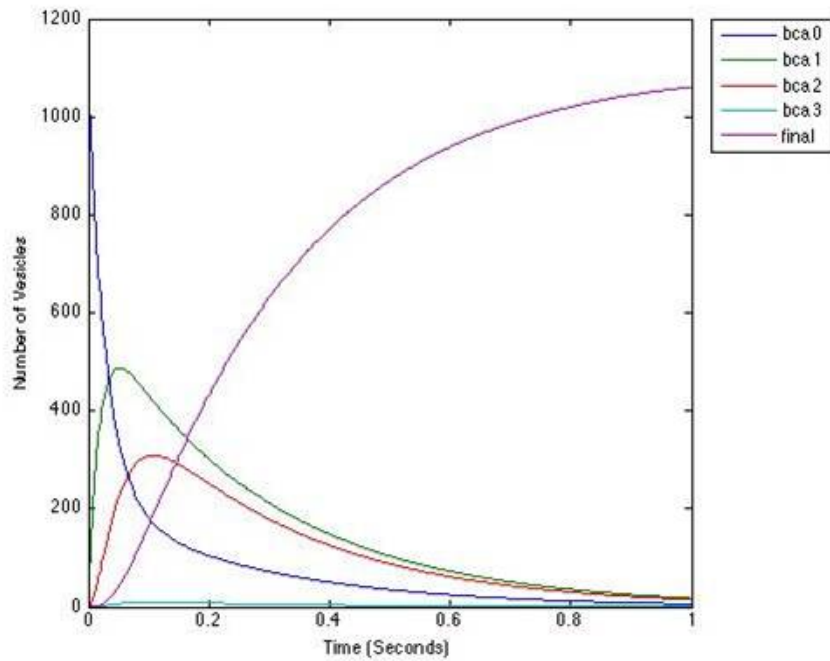


Figure 7. Three site fusion model.

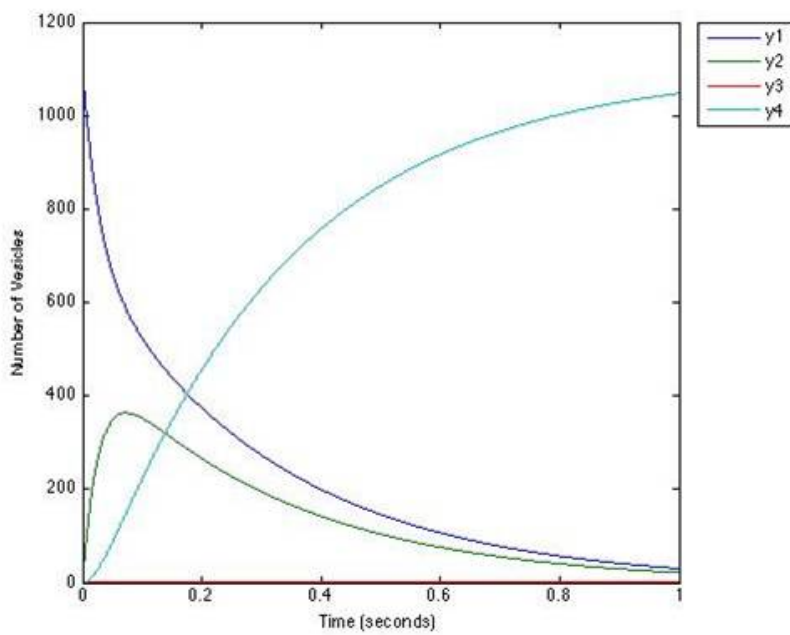


Figure 8. Two site fusion model.

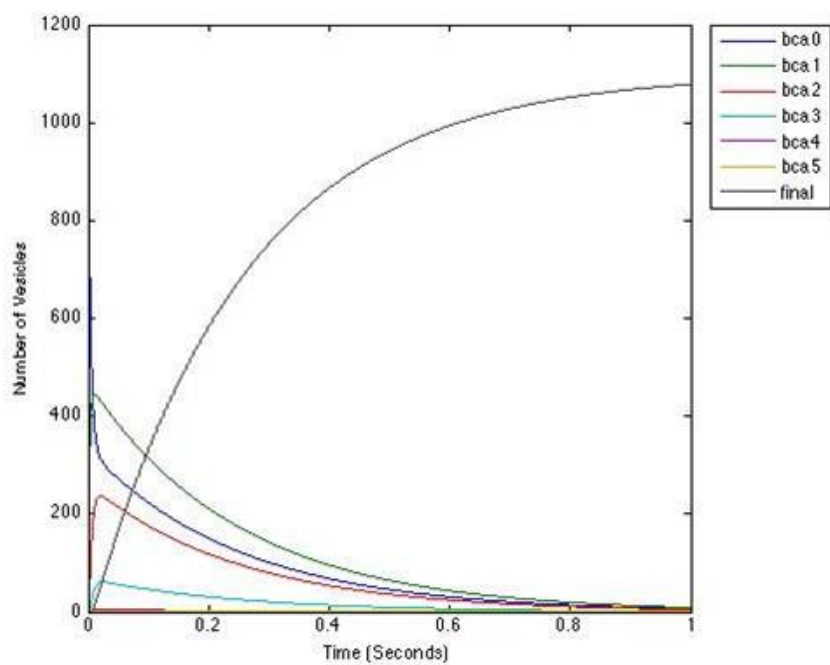


Figure 9. Five site allosteric fusion model.

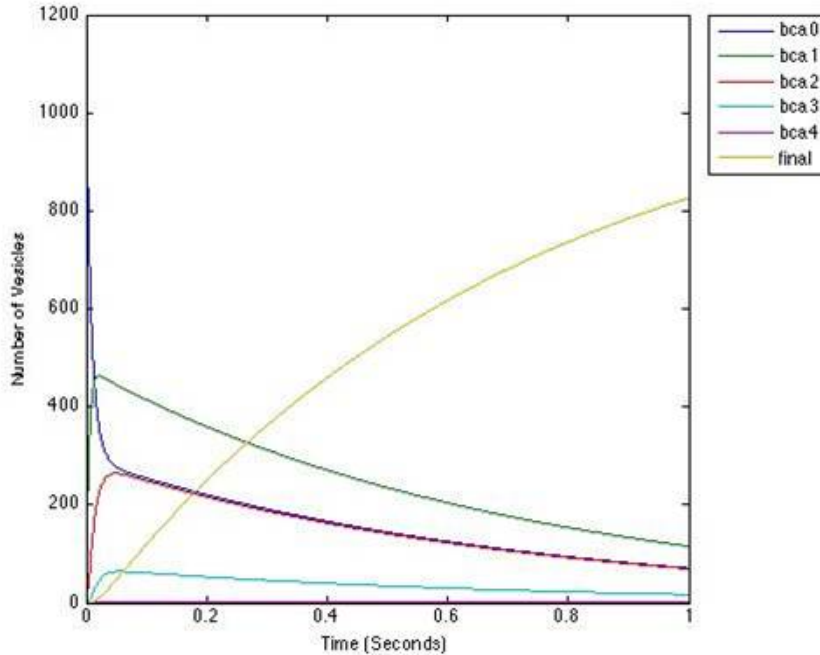


Figure 10. Four site fusion model.

4 Discussion

The curve of the final fuse pool qualitatively matches its expected shape. Notice that as the number of sites increases, the initial slope of the fuse pool curve tends to increase as well, except for the four site, which remains an anomaly. Further parameters from an inverse problem program are needed to compare the models further; however existing research shows that currently the 5-site allosteric provides the best match. However, any of the models are still viable options. The capacitance graphs are not included because they are simply linear multiples of the final fuse pool.

5 References

- [1] Heidelberg, R, *Electrophysiological approaches to the study of neuronal exocytosis and synaptic vesicle dynamics*. Rev Physiol Biochem Pharmacol. 2001;143:1-80.
- [2] Thoreson WB, Rabl K, Townes-Anderson E, Heidelberg R, A *highly Ca²⁺-sensitive pool of vesicles contributes to linearity at the*

rod photoreceptor ribbon synapse. Neuron. 2004 May 27;42(4):595-605.

- [3] Lou X, Scheuss V, Schneggenburger R, *Allosteric modulation of the presynaptic Ca²⁺ sensor for vesicle fusion*. Nature. 2005 May 26;435(7041):497-501.

6 Acknowledgements

1. Thanks to Dr. Heidelberger, Aron Goins, and the rest of the Heidelberger lab.
2. Additional thanks to Dr. Cox, Rice University, and the Gulf Coast Consortia for making this possible.
3. This work was partially supported by NSF REU Grant DMS-0755294.

7 Code

Attached in M-files.